AD-A046 803 NAVAL RESEARCH LAB WASHINGTON D C F/G 20/4
VISCOUS EFFECTS ON A ROTATING IMPLODING CYLINDRICAL LIQUID LINE--ETC(U)
SEP 77 A L COOPER, D L BOOK E(49-20)-1009
UNCLASSIFIED NRL-MR-3544 SBIE-AD-E000 010 NL

1 OF 1
AD A046 803

END
DATE FILMED
12-77
DDC

(12)

NRL Memorandum Report 3544

(6)

Viscous Effects on a Rotating Imploding Cylindrical Liquid Liner

(10) A. L. Cooper and D. L. Book

Plasma Physics Division

(9) Interim rept.,

(11) Sep[illegible]77

(12) 17 p.

(14) NRL-MR-3544

(15) E(49-2Φ)-1ΦΦ9

(18) SBIE

(19) AD-EΦΦΦ/ΦΙΦ

NAVAL RESEARCH LABORATORY
Washington, D.C.

251 950

-- 1 - AD NUMBER: [redacted]
-- 2 - FIELDS AND GROUPS: 20/4
-- 3 - CATALOG CARD CLASSIFICATION: UNCLASSIFIED
-- 4 - PRICES:
-- 5 - CORPORATE AUTHOR: NAVAL RESEARCH LAB WASHINGTON
-- D C
-- 6 - UNCLASSIFIED TITLE: VISCOUS EFFECTS ON A
-- ROTATING IMPLODING CYLINDRICAL LIQUID LINER.
-- 7 - CLASSIFIED TITLE:
-- 8 - TITLE CLASSIFICATION: UNCLASSIFIED
-- 9 - DESCRIPTIVE NOTE: INTERIM REPT.,
--10 - PERSONAL AUTHORS: COOPER,A. L. ;BOOK ,D. L. ;
--11 - REPORT DATE: SEP , 1977
--12 - PAGINATION: 16P
--14 - REPORT NUMBER: NRL-MR-3544
--15 - CONTRACT NUMBER: ERDA-E(49-20)-1009
--16 - PROJECT NUMBER:
--17 - TASK NUMBER:
--18 - MONITOR ACRONYM:
--19 - MONITOR SERIES:
--20 - REPORT CLASSIFICATION: UNCLASSIFIED

--21 - SUPPLEMENTARY NOTE:
--22 - LIMITATIONS (ALPHA): DISTRIBUTION OF DOCUMENT
-- CONTROLLED BY NAVAL RESEARCH LABORATORY, ATTN:
-- CODE 2628, WASHINGTON, D.C. 20375. THIS DOCUMENT
-- IS NOT AVAILABLE FROM DDC. CATALOGING INFORMATION
-- SUPPLIED BY NRL.
--23 - DESCRIPTORS: *VISCOSITY, *FLUID DYNAMICS,
-- BOUNDARY LAYER, LIQUID METALS, CYLINDERS,
-- IMPLOSIONS, LININGS, REYNOLDS NUMBER, ROTATION
--24 - DESCRIPTOR CLASSIFICATION: UNCLASSIFIED
--25 - IDENTIFIERS: *LIQUID LINERS, LPNH02-37
--26 - IDENTIFIER CLASSIFICATION: UNCLASSIFIED
--27 - ABSTRACT: THE EFFECT OF VISCOSITY ON THE INNER
-- SURFACE OF A ROTATING IMPLODING CYLINDRICAL
-- LIQUID METAL LINER IS ANALYZED IN THE LIMIT OF
-- HIGH REYNOLDS NUMBER RE. THE CONDITION OF
-- VANISHING TANGENTIAL STRESS ON THE FREE SURFACE
-- LEADS TO THE FORMATION OF A BOUNDARY LAYER OF
-- THICKNESS APPROXIMATELY RE TO THE MINUS 1/2 POWER.
-- THIS RESULTS IN A REQUIREMENT OF SLIGHTLY
-- INCREASED ROTATION IN ORDER TO SATISFY THE
-- CRITERION FOR SUPPRESSION OF THE RAYLEIGH-TAYLOR
-- INSTABILITY ON THE FREE SURFACE. FOR REYNOLDS
-- NUMBERS APPROPRIATE TO LIQUID METALS AND
-- PARAMETERS OF CURRENT EXPERIMENTAL INTEREST, THE
-- CORRECTION TO THE ROTATION REQUIRED FOR STABILITY
-- IS LESS THAN ONE PERCENT. CALCULATIONS ARE
-- PRESENTED FOR A MODEL LINEAR TRAJECTORY.
--28 - ABSTRACT CLASSIFICATION: UNCLASSIFIED
--29 - INITIAL INVENTORY: XXXXX
--30 - ANNOTATION:
--31 - SPECIAL INDICATOR:
--32 - REGRADE CATEGORY:
--33 - LIMITATION CODES: 1 21
--34 - SOURCE SERIES:
--35 - SOURCE CODE: 251950
--36 - DOCUMENT LOCATION: NRL
--37 - CLASSIFICATION AUTHORITY:
--38 - DECLASSIFICATION DATE:
--39 - DOWNGRADING DATE:
--40 - GEOPOLITICAL CODE: 1100
--41 - TYPE CODE: N
--42 - IAC ACCESSION NUMBER:
--43 - IAC DOCUMENT TYPE:
--44 - IAC SUBJECT TERMS:

SECURITY CLASSIFICATION OF THIS PAGE (When Data Entered)

REPORT DOCUMENTATION PAGE		READ INSTRUCTIONS BEFORE COMPLETING FORM
1. REPORT NUMBER NRL Memorandum Report 3544	2. GOVT ACCESSION NO.	3. RECIPIENT'S CATALOG NUMBER
4. TITLE (and Subtitle) VISCOUS EFFECTS ON A ROTATING IMPLODING CYLINDRICAL LIQUID LINER		5. TYPE OF REPORT & PERIOD COVERED Interim report on a continuing NRL problem. 6. PERFORMING ORG. REPORT NUMBER
7. AUTHOR(s) A. L. Cooper and D. L. Book		8. CONTRACT OR GRANT NUMBER(s) NRL Problem H02-37 Proj. No. ERDA-E(49-20)-1009 (81706)
9. PERFORMING ORGANIZATION NAME AND ADDRESS Naval Research Laboratory Washington, D.C. 20375		10. PROGRAM ELEMENT, PROJECT, TASK AREA & WORK UNIT NUMBERS
11. CONTROLLING OFFICE NAME AND ADDRESS Energy Research and Development Administration Washington, D.C. 20545		12. REPORT DATE 16 13. NUMBER OF PAGES September 1977
14. MONITORING AGENCY NAME & ADDRESS(if different from Controlling Office)		15. SECURITY CLASS. (of this report) UNCLASSIFIED 15a. DECLASSIFICATION/DOWNGRADING SCHEDULE

16. DISTRIBUTION STATEMENT (of this Report)

Approved for public release; distribution unlimited.

17. DISTRIBUTION STATEMENT (of the abstract entered in Block 20, if different from Report)

18. SUPPLEMENTARY NOTES

19. KEY WORDS (Continue on reverse side if necessary and identify by block number)
Liners
Viscosity
Boundary Layers
Fluid Dynamics

20. ABSTRACT (Continue on reverse side if necessary and identify by block number)

The effect of viscosity on the inner surface of a rotating imploding cylindrical liquid metal liner is analyzed in the limit of high Reynolds number *Re*. The condition of vanishing tangential stress on the free surface leads to the formation of a boundary layer of thickness $\sim Re^{-1/2}$. Within this layer the zonal velocity v is reduced by an amount Δv such that $\Delta v/v \sim Re^{-1/2}$. This results in a requirement of slightly increased rotation in order to satisfy the criterion for suppression of the Rayleigh-Taylor instability on the free surface. For Reynolds numbers appropriate to liquid metals
(Continued)

delta v

DD FORM 1 JAN 73 1473 EDITION OF 1 NOV 65 IS OBSOLETE
S/N 0102-LF-014-6601

SECURITY CLASSIFICATION OF THIS PAGE (When Data Entered)

* approx. 1/sq. root RE

20. Abstract (continued)

and parameters of current experimental interest, the correction to the rotation required for stability is less than one percent. Calculations are presented for a model linear trajectory.

CONTENTS

VISCOUS EFFECTS ON A ROTATING IMPLODING CYLINDRICAL LIQUID LINER

I. Introduction

Currently, there is a great deal of interest in the compression of magnetic fields and plasmas by means of the controlled implosion of highly electrically conducting hollow metallic cylinders (liners). The liners are launched by means of either high explosives,[1,2] electromagnetic inductive coupling,[3–6] or hydraulic compression[7]. The source energy which launches the liner is converted into kinetic energy of the liner and eventually into internal energy of the enclosed magnetic field-plasma mix. After the liner is stopped by the payload pressure (at the inner turning point), it rebounds and the energy is returned to the liner, which moves radially outward. Thus, the liner moves inward from the launch point to a minimum radius and maximum pressure condition at the inner turning point, and then back out again to the launch radius.

Different types of liner materials have been considered and launched upon purely magnetic field payloads as part of the NRL Linus program. These include solid Al and Cu liners and liquid metal liners of a sodium-potassium (NaK) eutectic mixture[7,8]. The current configurations utilize liquid metal liners.

For the early liners[8], a capacitor bank was used as an energy source and the liner had two free surfaces, the inside compression surface and an outer free surface. In an elementary fashion (detailed analytical and numerical analysis[9] substantiates this), it can be shown that the outer free surface is Rayleigh-Taylor unstable during the launch phase of the liner. The inner free surface is stable during this phase. However, in the vicinity of the inner turning point, the opposite is true: the inner free compression surface is Rayleigh-Taylor unstable, while the outer free surface is stable.

The inner free surface can be stabilized by liner rotation about the cylinder axis, which introduces a centripetal acceleration opposing $\ddot{R}$. With sufficient rotation, the inner surface can be stabilized throughout the entire liner trajectory. It would then be unstable only because of coupling to the outer surface during the launch phase. This, however, can be prevented by going to a "captive" liner[7] where the outer surface remains in contact with a set of axial or radial pistons driven by high pressure gas. This combination of rotation and hydraulic piston implosion leads to liners which are theoretically stable against Rayleigh-Taylor modes.

Manuscript submitted August 18, 1977.

While rotational stabilization of the inner free surface has been demonstrated theoretically[8] for an ideal inviscid liner and established experimentally,[9] the precise role of real liner fluid viscosity has remained an open question. In this paper we study the effects of liner viscosity in the realistic limit of large Reynolds number [experimental Reynolds numbers Re of the order of 2×10^4 are typical]. We find that viscous effects are concentrated in a thin boundary layer at the free surface whose thickness is of the order of $Re^{-1/2}$. The bulk of the liner behaves essentially inviscidly. Within the viscous boundary layer, the rotational speed of the liner at the free surface is reduced from that which would occur inviscidly. The boundary layer thickness and reduction in angular velocity are determined as quadratures of the basic state trajectory, $R(t)$. Numerical results are obtained for a model prescribed radial trajectory and presented as a function of the compression ratio and Reynolds number.

II. Analytical Treatment

The liquid liner is assumed to undergo a cylindrical flow corresponding to the motion of an infinite hollow cylinder which is imploding while rotating about its axis. Rotation is necessary both for the initial formation of the liner and to stabilize against the Rayleigh-Taylor instabilities near the inner turning point. In this study we will concentrate on the inner free surface and, without any essential change in the physics, will consider the liner to be infinitely thick.

The following assumptions are made:

1. The liner is launched from a state of rigid rotation with angular velocity, Ω_0, at time $t = 0$.
2. The liner is incompressible (constant density ρ).
3. The liner kinematic viscosity ν is constant.
4. The flow is laminar.
5. The flow is one dimensional $\left(\frac{\partial}{\partial \phi} = \frac{\partial}{\partial z} = 0\right)$.
6. Surface tension is neglected.

Incompressibility of the liner in this case implies

$$\frac{\partial}{\partial r}(ru) = 0, \tag{1}$$

where $u(r,t)$ is the radial velocity component. The radial component of the Navier-Stokes equation governs the radial motion,

$$\frac{\partial u}{\partial t} + u\frac{\partial u}{\partial r} - \frac{v^2}{r} + \frac{1}{\rho}\frac{\partial p}{dr} = \nu \frac{\partial}{\partial r}\left[\frac{1}{r}\left(\frac{\partial ru}{\partial r}\right)\right], \tag{2}$$

where $v(r,t)$ is the zonal velocity and $p(r,t)$ is the pressure. The angular momentum equation, which is formed from the zonal component of the Navier-Stokes equation, is given as

$$\frac{\partial rv}{\partial t} + u\frac{\partial}{\partial r}(rv) = \nu r \frac{\partial}{\partial r}\left[\frac{1}{r}\frac{\partial}{\partial r}(rv)\right]. \tag{3}$$

Substitution of Eq. (1) into Eq. (2) reveals that the right-hand side of the radial momentum equation vanishes. Viscous effects arise only through coupling with the zonal momentum

equation (3) by virtue of the centripetal acceleration term, $-v^2/r$. An additional viscous effect arises at the free surface, where the normal stress is balanced. This will be discussed later in the paper when we consider the boundary conditions.

The coupled Eqs. (1-3) should be solved consistent with proper initial and boundary conditions to provide $u(r,t)$, $v(r,t)$ and $p(r,t)$. In order to emphasize the main physics of this problem in its most simple form, we will instead consider the radial trajectory of the liner to be prescribed, and generate consistent solutions to the angular momentum equation. The viscous evolution of the angular momentum distribution is direct, while the viscous effects upon the radial velocity field are mainly a result of the coupling to the zonal equation through the centripetal acceleration term, $-(rv)^2/r^3$.

A. *Radial Trajectory*

We therefore consider a prescribed radial trajectory of the free surface

$$R = R(t/t_0; \epsilon), \tag{4}$$

where t_0, the hydrodynamic time, represents the throw time (time required to go from the initial radius $R_0 \epsilon^{-1/2}$ to the minimum radius R_0), and $\epsilon^{1/2}$ represents the ratio of minimum to maximum radius (compression ratio). These dimensions and parameters are indicated in Fig. 1.

Integrating the continuity equation (1) we obtain

$$ru = R\,dR/dt = K(t), \tag{5}$$

i.e., ru is a constant throughout the liner at any given time t. Therefore, the specification of the free surface trajectory, Eq. (4), completely defines the entire radial velocity field.

The general approach applied in this study is valid for an arbitrary trajectory. For this study, however, we take a "parabolic" form for the prescribed trajectory

$$\left(\frac{R}{R_0}\right)^2 = 1 + \left(\frac{1}{\epsilon} - 1\right)\left(1 - \frac{t}{t_0}\right)^2. \tag{6}$$

It can be shown that this type of trajectory represents a realistic limit of a *thin* freely launched liner, $\Delta/R << 1$, where Δ is the liner thickness. The numerical results to be presented in this study will be associated with this trajectory. For strict consistency with our previous approximation that the outer radius is at infinity, it is necessary that viscous effects be confined to a layer of thickness $\delta << \Delta$.

B. *Initial and Boundary Conditions*

We desire a solution to Eq. (3) with the prescribed trajectory given by Eq. (6). Since the liner is launched from a rigid rotation state with angular velocity Ω_0, the initial condition on $A(r,t) = rv$ is

$$A(r,0) = r^2\Omega_0,\ r \geq R_0\epsilon^{-1/2}. \tag{7}$$

A suitable boundary condition must also be applied at the free surface, $r = R(t)$. The free surface is an interface between a liquid and a magnetic field or magnetic field-plasma mixture. In either case, there should be negligible tangential shear stress $\Sigma_{r\phi}$ at the free surface, and the normal stress in the liquid liner should be in balance with the plasma and/or magnetic pressure p_i of the interior volume there. Therefore at the interface,

$$\sigma_{r\phi} = \rho\nu r \frac{\partial}{\partial r}\left(\frac{A}{r^2}\right) = 0; \tag{8}$$

$$p - \nu\rho \frac{\partial u}{\partial r} = p_i. \tag{9}$$

The vanishing of the tangential shear stress prescribed by Eq. (8) implies that at $r = R(t)$ the angular momentum satisfies

$$A = Cr^2. \tag{10}$$

Thus the zonal velocity field is locally that of a rigid body rotation with arbitrary angular velocity given by the integration constant C, which is in general a function of time.

We notice that the boundary condition, Eq. (8), is satisfied by the initial condition, Eq. (7), which specifies that the liner is launched from a state of rigid rotation.

Equations (7) and (8) provide one initial condition and one boundary condition for the angular momentum equation, Eq. (3). An additional boundary condition is required since we have a second order equation in r. This second boundary condition arises as a far-field condition in the liner for $r > R$. To see this more clearly, we observe that the inviscid solution ($\nu = 0$) of Eq. (3), subject to the initial condition, Eq. (7), satisfies the full viscous equation, but not the boundary condition, Eq. (8). We therefore anticipate that far from the free surface, $r >> R$, the liner will behave inviscidly. A viscous boundary layer will exist at the free surface which recovers the boundary condition, Eq. (8), at the free surface and matches with the inviscid solution in the interior of the liner. This matching condition provides the second required boundary condition.

Figure 2 illustrates the nature of this viscous boundary layer. The liner is shown launched at time $t = 0$ with a solid-body rotation corresponding to that of the apparatus, Ω_0. The liner is also depicted at a later time, t, after it has imploded to a radius $R(t)$. The inviscid zonal velocity variation appropriate at that time is indicated by the solid line. This variation corresponds to conservation of specific angular momentum rv for each of the fluid lamellae composing the liner. The viscous layer or boundary layer correction is shown in the region δ by means of the dashed line. The viscous solution satisfies the stressless condition at the surface and matches with the inviscid distribution in the interior. Viscosity is seen to slow down the liner interface zonal velocity. This is important, as we rely on the strong zonal motion of the inside surface in the vicinity of the turning point to stablize against Rayleigh-Taylor instabilites.

C. *Lagrangian Variables*

Because of the motion of the free surface and the inherent competition between convection with geometric convergence and diffusion displayed by Eq. (3), it is more convenient to transform to Lagrangian variables. We therefore take

$$\xi = r^2 - R^2(t), \tag{11}$$

which is proportional to the displaced area relative to the moving interface and is conserved for fluid shells in an incompressible liner. This transformation has been used previously by the present authors in a related problem [11].

The angular momentum equation for $A(\xi,t)$ becomes

$$\frac{\partial A}{\partial t} = 4\nu \left[R^2(t) + \xi\right] \frac{\partial^2 A}{\partial \xi^2}, \tag{12}$$

with initial and boundary conditions

$$A(\xi,0) = \left[R^2(0) + \xi\right] \Omega_0, \tag{13}$$

$$\frac{\partial A}{\partial \xi}(0,t) = \frac{A(0,t)}{R^2(t)} \tag{14}$$

and for $\xi \to \infty$,

$$A(\xi,t) \sim \Omega_0 \left[\xi + R^2(0)\right]. \tag{15}$$

Equation (15) requires that the solution match with the inviscid solution far into the liner.

D. *Nondimensionalization*

The dependent and independent variables are normalized as follows:

$$\tilde{A} = A/R_0^2 \Omega_0, \quad \tilde{t} = t/t_0,$$

$$\tilde{R} = R/R_0, \quad \tilde{\xi} = \xi/R_0^2.$$

Two dimensionless parameters characterize the problem:

$$\epsilon = \frac{R_0^2}{R^2(0)}; \tag{17}$$

$$\mathrm{Re} = R_0^2/4\nu t_0. \tag{18}$$

Re, a Reynolds number, represents the ratio of the viscous diffusion time $R_0^2/4\nu$ to the hydrodynamic time associated with the prescribed radial motion, t_0. Since this is a boundary layer problem, we anticipate that the viscous zone will scale as $\mathrm{Re}^{-1/2}$. As previously defined, ϵ is an inverse compression ratio representing the ratio of the final compression area to its initial value for the prescribed trajectory. In terms of these non-dimensional variables, the relevant equations and initial and boundary conditions become

$$\frac{\partial \tilde{A}}{\partial \tilde{t}} = \frac{1}{\mathrm{Re}} \left[\tilde{R}^2(t) + \tilde{\xi}\right] \frac{\partial^2 A}{\partial \tilde{\xi}^2}; \tag{19}$$

$$\tilde{A}(\tilde{\xi},0) = \tilde{R}^2(0) + \tilde{\xi}; \tag{20}$$

$$\frac{\partial \tilde{A}}{\partial \tilde{\xi}}(0,\tilde{t}) = \frac{\tilde{A}(0,\tilde{t})}{\tilde{R}^2(\tilde{t})}, \tag{21}$$

and

$$\tilde{A}(\tilde{\xi},\tilde{t}) \sim \tilde{\xi} + \frac{1}{\epsilon}, \tag{22}$$

at large ξ, where

$$\tilde{R}^2(\tilde{t}) = 1 + \left[\frac{1}{\epsilon} - 1\right](1 - \tilde{t})^2 \tag{23}$$

A solution to Eqs. (19-23) valid throughout $\mathrm{Re} - \epsilon$ parameter space represents a formidable task. For large values of Re, the situation is significantly simplified. This limit is also of practical interest, as the Reynolds numbers associated with magnetic compression using NaK liners are of the order of 2×10^4.

E. *Asymptotic Theory at Large Reynolds Number*

We concentrate on the large-Reynolds-number portion of the Re $-\epsilon$ parameter space. In particular, we seek the behavior of Eq. (19-23) in the following asymptotic limit:

$$\mathrm{Re}^{-1/2} << \epsilon \leqslant 1, \tag{24}$$

and will apply the methods of matched asymptotic analysis to Eqs. (19-23), taking advantage of the small parameter $\mathrm{Re}^{-1/2}$. Henceforth, we omit the tilde from dependent and independent variables, with the understanding that all variables are dimensionless.

a. *Outer Solution*

We expand the angular momentum A in a regular perturbation expansion in terms of the small parameter $Re^{-1/2}$:

$$A(\xi,t;\mathrm{Re},\epsilon) \sim A^{(0)}(\xi,t;\epsilon) + \mathrm{Re}^{-1/2}A^{(1)}(\xi,t;\epsilon) + \cdots . \tag{25}$$

To lowest order in $\mathrm{Re}^{-1/2}$, Eqs. (19-23) become

$$\frac{\partial A^{(0)}}{\partial t} = 0, \tag{26}$$

with

$$A^{(0)}(\xi,0) = \xi + \frac{1}{\epsilon}, \tag{27}$$

$$\frac{\partial A^{(0)}}{\partial \xi}(0,t) = \frac{A^{(0)}}{R^2(t)}, \tag{28}$$

and

$$A^{(0)}(\xi,t) \sim \xi + \frac{1}{\epsilon} \tag{29}$$

at large ξ. The solution to Eq. (26) which satisfies Eqs. (27) and (29) is

$$A^{(0)}(\xi,t;\epsilon) = \xi + \frac{1}{\epsilon}. \tag{30}$$

This solution does not, however, satisfy the required stressless boundary condition, Eq. (28). We therefore have the ingredients for a classical boundary layer. It is necessary to rescale the independent variable ξ to recover the missing boundary condition and resolve this layer.

b. *Inner Solution*

The necessary stretching of ξ is given as

$$\eta = \mathrm{Re}^{1/2}\xi, \tag{31}$$

and the dependent variable is written as

$$\hat{A} = \hat{A}(\eta,t;\epsilon). \tag{32}$$

In terms of Eqs. (31) and (32), the governing equations, Eqs. (19-23), become

$$\frac{\partial \hat{A}}{\partial t} = [R^2(t) + \eta\,\mathrm{Re}^{-1/2}]\frac{\partial^2 \hat{A}}{\partial \eta^2}; \tag{33}$$

$$\hat{A}(\eta,0) = \frac{1}{\epsilon} + \eta\mathrm{Re}^{-1/2}; \tag{34}$$

$$\frac{\partial \hat{A}}{\partial \eta}(0,t) = \mathrm{Re}^{-1/2} \frac{\hat{A}(0,t)}{R^2(t)}; \tag{35}$$

$$\hat{A}(\eta,t) \sim \frac{1}{\epsilon} + \eta \mathrm{Re}^{-1/2}, \eta >> 1. \tag{36}$$

The initial and boundary conditions satisfied by Eqs. (34) and (36) are evidently the inner representation of the inviscid solution and satisfy the differential equation Eq. (33). It is therefore convenient to define a new angular momentum variable by means of

$$\bar{A}(\eta,t;\epsilon) = \hat{A}(\eta,t;\epsilon) - \left[\frac{1}{\epsilon} + \eta \mathrm{Re}^{-1/2}\right]. \tag{37}$$

$\bar{A}(\eta,t;\epsilon)$ represents the viscous correction to the solution. Equations (33-36) become

$$\frac{\partial \bar{A}}{\partial t} = [R^2(t) + \eta \mathrm{Re}^{-1/2}] \frac{\partial^2 \bar{A}}{\partial \eta^2} \tag{38}$$

with

$$\bar{A}(\eta,0) = 0, \tag{39}$$

$$\frac{\partial \bar{A}}{\partial \eta}(0,t) = \mathrm{Re}^{-1/2}\left[\frac{\bar{A}(0,t) + \frac{1}{\epsilon}}{R^2(t)} - 1\right], \tag{40}$$

and

$$\lim_{\eta \to \infty} \bar{A}(\eta,t) = 0. \tag{41}$$

We now expand $\bar{A}$ as a regular perturbation expansion in powers of the small parameter $\mathrm{Re}^{-1/2}$:

$$\bar{A}(\eta,t;\mathrm{Re},\epsilon) \sim \bar{A}^{(0)}(\eta,t;\epsilon) + \mathrm{Re}^{-1/2}\bar{A}^{(1)}(\eta,t;\epsilon) + \cdots \tag{42}$$

To lowest order in $\mathrm{Re}^{-1/2}$ we find that

$$\bar{A}^{(0)} = 0, \tag{43}$$

and to next order we obtain

$$\frac{\partial \bar{A}^{(1)}}{\partial t} = R^2(t) \frac{\partial^2 \bar{A}^{(1)}}{\partial \eta^2} \tag{44}$$

with

$$\bar{A}^{(1)}(\eta,0) = 0, \tag{45}$$

$$\frac{\partial \bar{A}^{(1)}}{\partial \eta}(0,t) = 1/\epsilon\, R^2(t) - 1, \tag{46}$$

and

$$\lim_{\eta \to \infty} \bar{A}^{(1)}(\eta,t) = 0, \tag{47}$$

Defining a new timelike variable, the age,

$$\theta = \int_0^t R^2(t')dt', \tag{48}$$

reduces Eq. (44) to a diffusion equation which is identical to that governing diffusion in a slab,

$$\frac{\partial \bar{A}^{(1)}}{\partial \theta} = \frac{\partial^2 \bar{A}^{(1)}}{\partial \eta^2}. \tag{49}$$

It should be borne in mind that η is a dimensionless area and θ is a stretched time variable which is weighted over the trajectory. That is, even though Eq. (49) has the form of a slab diffusion, it still includes effects of geometric convergence consistent with the liner motion asymptotically correctly for the large Reynolds number considered here.

The solution to Eq. (49) with the conditions of Eqs. (45-47) is written as

$$\bar{A}^{(1)}(\eta,\theta;\epsilon) = -\frac{1}{\sqrt{\pi}} \int_0^{\theta} \frac{d\tau e^{-\eta^2/4(\theta-\tau)}}{(\theta-\tau)^{1/2}} [1/\epsilon R^2(\tau) - 1]. \tag{50}$$

Equation (50), the viscous correction to the angular momentum, is given as a quadrature over the basic state trajectory $R(\tau)$. That is, $\bar{A}^{(1)}$ is a function not only of the compression ratio ϵ, but of the details of the full trajectory in terms of the age defined in Eq. (48).

In summary, the angular momentum distribution is from Eqs. (37) and (50)

$$\hat{A}(\eta,t;\mathrm{Re},\epsilon) \sim \left[\frac{1}{\epsilon} + \eta\,\mathrm{Re}^{-1/2}\right] - \mathrm{Re}^{-1/2} \frac{1}{\sqrt{\pi}} \int_0^{\theta} \frac{d\tau e^{-\eta^2/4(\theta-\tau)}}{(\theta-\tau)^{1/2}} (1/\epsilon R^2 - 1). \tag{51}$$

Of particular interest is the angular momentum at the free surface. This is basic to stabilization of the Rayleigh-Taylor instability which could occur near the inner turning point $t = t_0$. Taking $\eta \to 0$ we find

$$\hat{A}(0,t;\mathrm{Re},\epsilon) \sim \frac{1}{\epsilon} - \mathrm{Re}^{-1/2} \frac{1}{\sqrt{\pi}} \int_0^{\theta} \frac{d\tau}{(\theta-\tau)^{1/2}} \left[\frac{1}{\epsilon R^2(\tau)} - 1\right]. \tag{52}$$

Therefore, the angular velocity of the free surface is given as

$$\frac{\Omega}{\Omega_0} = \frac{1}{R^2(\theta)} \left\{\frac{1}{\epsilon} - \mathrm{Re}^{-1/2} \int_0^{\theta} \frac{d\tau}{(\theta-\tau)^{1/2}} \left[\frac{1}{\epsilon R^2(\tau)} - 1\right]\right\} \tag{53}$$

or

$$\frac{\Omega}{\Omega_{inv}} = 1 - \mathrm{Re}^{-1/2} \epsilon \int_0^{\theta} \frac{d\tau}{(\theta-\tau)^{1/2}} \left[\frac{1}{\epsilon R^2(\tau)} - 1\right] \equiv 1 - \mathrm{Re}^{-1/2} f(t,\epsilon) \tag{54}$$

where $\Omega_{inv} = \Omega_0/\epsilon R^2$ is the inviscid surface angular velocity. The reduction in angular velocity of the free surface from its inviscid value is seen to scale as $\mathrm{Re}^{-1/2}$.

III. RESULTS

In this section we discuss some of the results obtained for this application. Particular emphasis will be placed on the viscous pertubation of the free-surface angular velocity, since this quantity is most important in stable and well-controlled basic state motion.

The quadratures required to evaluate the scaled specific angular momentum profile [Eq. (51)] were performed numerically. The integration variable was taken to be t instead of θ, using the transformation $d\theta = dt\,(d\theta/dt)$ and evaluating $d\theta/dt$ by Eq. (48). Dividing the range of integration into 10^4 equal-time intervals and using the trapezoid rule yielded results accurate

to $\sim$ 1%. Landen's transformation[11] was used to evaluate the incomplete elliptic integral which results when parabolic trajectories [Eq. (23)] are employed in Eq. (54).

In Fig. 3, f as defined in Eq. (54), the viscous correction to the free surface angular velocity, is plotted as a function of time for various values of ϵ. The viscous reduction in surface angular velocity is seen to evolve from zero at $t = 0$ and increase with time, slowly at first, and then rapidly near the inner turning point, $t = 1$. The maximum value, of order 1 in all cases, is obtained shortly after the turning point for this model trajectory. As the liner moves outward towards its maximum radius at $t = 2$, the correction decreases. The correction does not vanish entirely, however, even at $t = 2$ when the liner has returned to its initial radius. Figure 3 shows that there is signficant ϵ dependence in the effects produced by finite viscosity. In particular, we see that f tends to decrease as $\epsilon \to 0$. It can be shown in this limit that for $t \neq 1$,

$$f(t;\epsilon) \sim \epsilon^{1/2}, \tag{55}$$

while

$$f(1;\epsilon) \sim \epsilon^{1/4}, \tag{56}$$

provided inequality (24) continues to hold.

At turnaround, where rotational stabilization is most critical,

$$\lim_{\epsilon \to 0} \epsilon^{-1/4} f(1;\epsilon) = 2.44. \tag{57}$$

Therefore from Eq. (54),

$$(\Omega_{inv} - \Omega)/\Omega_{inv} \simeq 2.44 \mathrm{Re}^{-1/2} \epsilon^{1/4} = 2.44\,(\mathrm{Re})_{eff}^{-1/2}, \tag{58}$$

where

$$(\mathrm{Re})_{eff} = R_0 R_{\max}/4\nu t_0 \tag{59}$$

is an effective Reynolds number related to both the minimum and maximum radii of the trajectory.

But it is also clear that

$$\lim_{\epsilon \to 1} f(t;\epsilon) = 0. \tag{60}$$

The behavior in both limits is shown in Fig. 4a, where we plot the surface angular velocity correction at $t = 1$ as a function of ϵ. Figure 4b shows the same curve, scaled by $\epsilon^{-1/4}$ to exhibit the asymptotic dependence of Eq. (56).

For liquid alkali metals, a typical viscosity is $\nu \simeq 1$ centipose. Taking $t_0 \simeq 10^{-3}$ sec, $R_0 = 1$ cm and $\epsilon = 10^{-3}$ yields $(\mathrm{Re})_{eff}^{-1/2} \simeq 10^{-3}$. Thus the relative change in surface angular velocity due to viscous effects is always less than one percent in cases of practical interest.

IV. SUMMARY

Viscous effects for imploding liners at large ratios of viscous diffusion time to hydrodynamic time (high Reynolds number) are confined to thin boundary layers near the stressless free surface. The boundary layer thickness scales as $\mathrm{Re}^{-1/2}$, with the interior region of the liner behaving inviscidly. The resulting problem has been solved by the methods of matched asymptotic analysis. A boundary layer structure has been obtained which satisfies equations identical to those associated with one-dimensional slab diffusion while properly including the

effects of geometrical convergence. The results obtained indicate that the free surface angular momentum is reduced from its inviscid value by an amount proportional to $Re^{-1/2}$.

REFERENCES

1. C. M. Fowler, W. B. Garn and R. S. Caird, J. Appl. Phys. **31**, 588 (1960).
2. A. D. Sakharov, R. Z. Lyudaev, E. N. Smirnov, Yu. I. Plyushchev, A. J. Pavlovskii, V. K. Chernyshev, A. E. Feoktistova, E. J. Zharinov, and Yu. A. Zysin, Dohl. Akad. Nauk USSR **165**, 65 (1965) [Sov. Phys. - Doyl. **10**, 1045 (1966)].
3. E. C. Cnare. J. Appl. Phys. **37**, 3812 (1966).
4. S. G. Alikhanov, V. G. Belan, G. J. Budker, A. J. Ivanchenkov and G. N. Kichigin, At. Energ. **23**, 536 (1967) [Sov. J. At. Energy **23**, 1507 (1967)].
5. J. Besancon, J. Morin and J. Vedel, C. R. Acad. Sci. **B267**, 1319 (1968).
6. S. G. Alikhanov, V. P. Bakhtin, V. M. Brusnikin, I. S. Glushkov, R. Kh. Kurtmullaev, A. L. Lumin, A. D. Mazychenko, V. P. Novikov, V. V. Pichygin, V. N. Simenov, G. E. Smolkin, E. G. Utyugov and I. Ya. Shipuk, Proc. 6th Int. Conf. on Plasma Physics and Controlled Thermonuclear Fusion Research, Berchtengaden, FGR, October 1976 (IAEA Vienna, to be published), paper No. E-19-2.
7. D. L. Book, A. L. Cooper, R. Ford, D. Hammer, D. J. Jenkins, A. E. Robson, P. J. Turchi, Proc. 6th Int. Conf. on Plasma Physics and Controlled Nuclear Fusion Research, Berchtesgaden, FGR, Oct. 1976 (IAA, Vienna, to be published), paper No. E-19-1.
8. P. J. Turchi, A. L. Cooper, R. Ford and D. J. Jenkins, Phys. Rev. Lett. **36**, 1546 (1976).
9. A. Barcilon, D. L. Book. and A. L. Cooper, Phys. Fluids **17**, 1707 (1974).
10. A. L. Cooper and D. L. Book, "Diffusion of Magnetic Flux Into a Cylindrical Liner is The Limit of High Magnetic Reynolds Number," NRL Memo. Rept. No. 3507 (1977).
11. M. Abramowitz and I. Stegun (editors), *Handbook of Mathematical Functions* (Dover Publications, New York, 1970) p. 597.

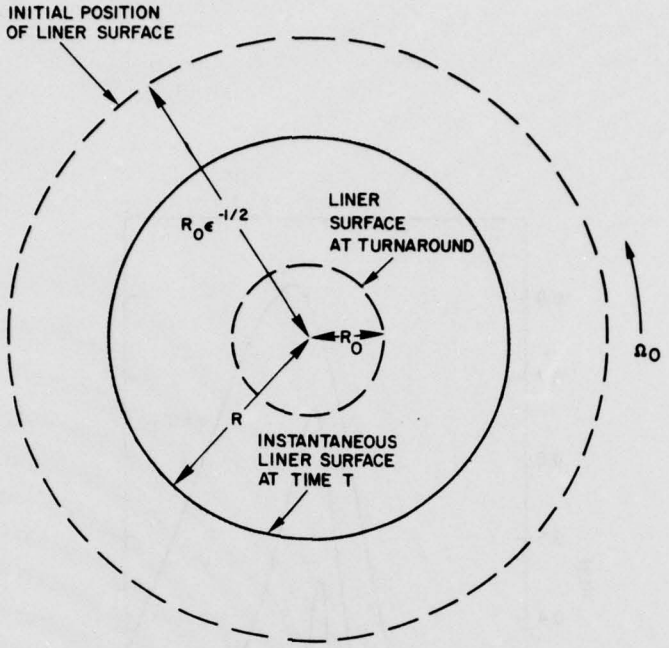

Fig. 1 — Geometry of the model used to study viscous effects at the free surface of a rotating imploding liner.

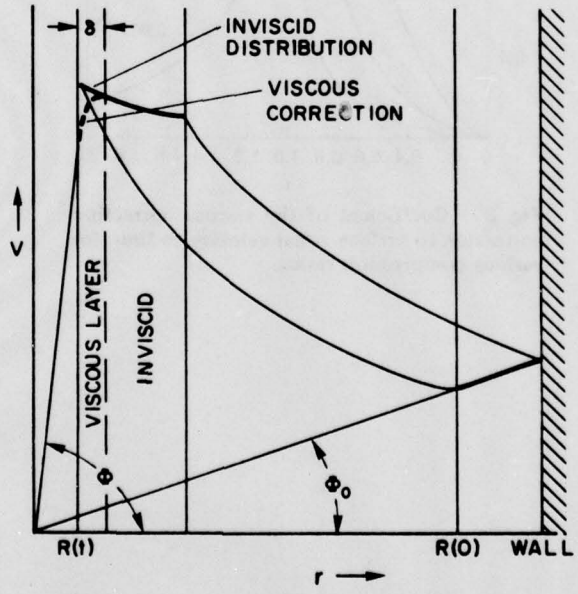

Fig. 2 — Schematic representation of the viscous boundary layer at the free surface of the liner, showing the reduction in surface zonal velocity resulting from the condition of zero tangential shear stress.

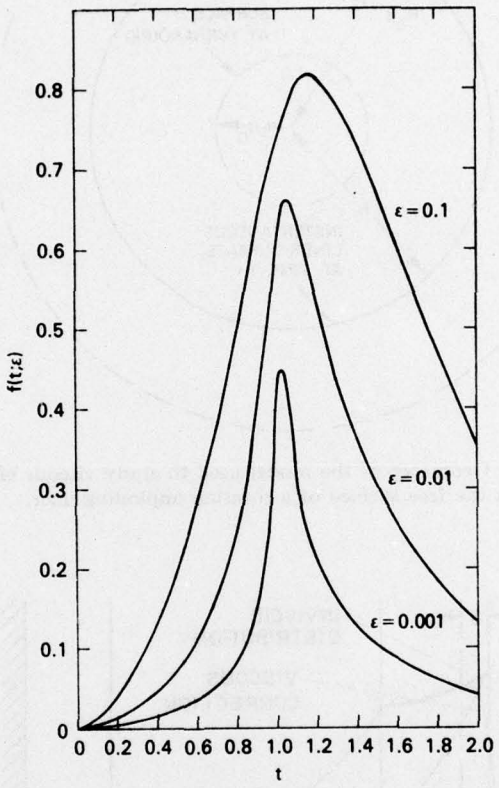

Fig. 3 — Coefficient of the viscous correction correction to surface zonal velocity vs time for various compression ratios.

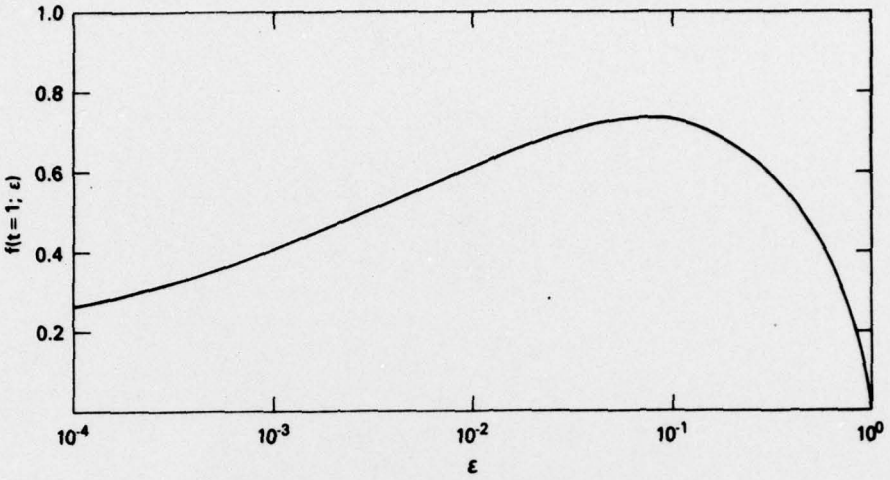

Fig. 4(a) — Plot of the viscous correction coefficient [Eq. (54)] at turnaround $f(1;\epsilon)$ vs ϵ.

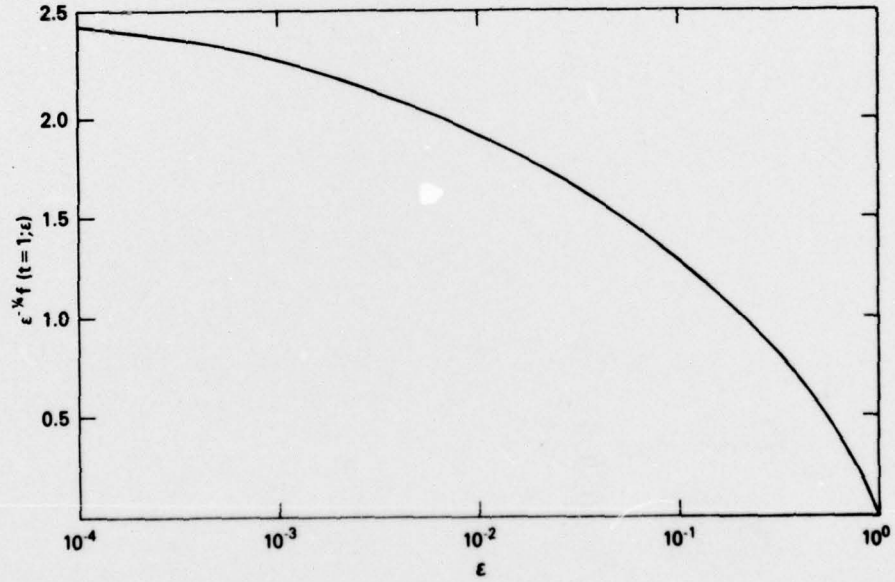

Fig. 4 (b) — Plot of $\epsilon^{-1/4} f(1;\epsilon)$, showing the asymptotic behavior $f(1;\epsilon) \sim \epsilon^{1/4}$ at small ϵ.